



The impact of unilateral pulmonary artery stenosis on right ventricular to pulmonary arterial coupling in patients with transposition of the great arteries

Renée S. Joosen MSc¹  | Michiel Voskuil MD, PhD² |
 Gregor J. Krings MD, PhD¹  | M. Louis Handoko MD, PhD³ |
 Michael G. Dickinson MD, PhD² | Marielle C. van de Veerdonk MD, PhD³ |
 Johannes M. P. J. Breur MD, PhD¹

¹Department of Pediatric Cardiology, University Medical Center Utrecht, Utrecht, The Netherlands

²Department of Cardiology, University Medical Center Utrecht, Utrecht, The Netherlands

³Department of Cardiology, Amsterdam University Medical Centers, Amsterdam Cardiovascular Sciences, University of Amsterdam, Amsterdam, The Netherlands

Correspondence

Johannes M. P. J. Breur, MD, PhD, Department of Pediatric Cardiology, University Medical Center Utrecht, Heidelberglaan 100, 3584 CX Utrecht, The Netherlands.
 Email: h.breur@umcutrecht.nl

Funding information

Stichting Hartekind; Hartstichting

Abstract

Background: Unilateral pulmonary artery (PA) stenosis is common in the transposition of the great arteries (TGA) after arterial switch operation (ASO) but the effects on the right ventricle (RV) remain unclear.

Aims: To assess the effects of unilateral PA stenosis on RV afterload and function in pediatric patients with TGA-ASO.

Methods: In this retrospective study, eight TGA patients with unilateral PA stenosis underwent heart catheterization and cardiac magnetic resonance (CMR) imaging. RV pressures, RV afterload (arterial elastance [Ea]), PA compliance, RV contractility (end-systolic elastance [Ees]), RV-to-PA (RV-PA) coupling (Ees/Ea), and RV diastolic stiffness (end-diastolic elastance [Eed]) were analyzed and compared to normal values from the literature.

Results: In all TGA patients (mean age 12 ± 3 years), RV afterload (Ea) and RV pressures were increased whereas PA compliance was reduced. RV contractility (Ees) was decreased resulting in RV-PA uncoupling. RV diastolic stiffness (Eed) was increased. CMR-derived RV volumes, mass, and ejection fraction were preserved.

Conclusion: Unilateral PA stenosis results in an increased RV afterload in TGA patients after ASO. RV remodeling and function remain within normal limits when analyzed by CMR but RV pressure–volume loop analysis shows impaired RV diastolic stiffness and RV contractility leading to RV-PA uncoupling.

KEYWORDS

cardiac magnetic resonance imaging, pulmonary pressures, pulmonary stenosis, right ventricular dysfunction, transposition of the great arteries

Marielle C. van de Veerdonk and Johannes M. P. J. Breur shared last authorship.

This is an open access article under the terms of the [Creative Commons Attribution-NonCommercial](https://creativecommons.org/licenses/by-nc/4.0/) License, which permits use, distribution and reproduction in any medium, provided the original work is properly cited and is not used for commercial purposes.

© 2024 The Authors. *Catheterization and Cardiovascular Interventions* published by Wiley Periodicals LLC.

1 | INTRODUCTION

Unilateral pulmonary artery (PA) stenosis is common in the transposition of the great arteries (TGA) after arterial switch operation (ASO).¹ This results in increased blood flow to the unobstructed contralateral PA, ventilation-perfusion mismatch, reduced ventilatory efficiency, and reduced exercise capacity.² The effects on right ventricle (RV) afterload and function remain unknown but is of great importance since RV maladaptation leads to reduced RV function, RV failure, and poor prognosis.^{3–5} RV pressure–volume (PV) loop analysis assessing RV-to-PA (RV-PA) coupling is considered the gold standard to evaluate RV adaptation in relationship to RV afterload and to predict maladaptive remodeling.⁶ This study explores the effects of unilateral PA stenosis on RV afterload and its relationship with RV function in patients with TGA after ASO using heart catheterization, cardiac magnetic resonance (CMR) imaging, and RV PV loop analysis.

2 | METHODS

Nineteen TGA patients underwent heart catheterization for unilateral PA stenosis after ASO at the University Medical Center Utrecht, The Netherlands, between 2009 and 2021. Patients were included if they underwent CMR within 6 months before heart catheterization. Twelve out of 19 patients were, therefore, included. Four out of 12 patients did not have properly stored RV pressure curves to perform RV PV loop analysis and were excluded. Therefore, eight patients were analyzed and results were compared to normal values from literature.^{7–12} Patients underwent regular clinical follow-up. Six out of eight patients underwent CMR and five out of eight patients underwent cardiopulmonary exercise testing (CPET) during follow-up. All subjects gave written informed consent.

2.1 | Heart catheterization

Heart catheterization was performed under conscious sedation. During invasive right and left-sided heart catheterization, pressures were measured in the right atrium, RV, mean PA, left PA (LPA), right PA (RPA), left atrium, left ventricle (LV), and aorta. Pulmonary artery compliance (PAC) was calculated as the ratio of stroke volume to pulmonary pulse pressure.¹¹

2.2 | CMR imaging

All CMR images were acquired using a 1.5 Tesla scanner (Philips Medical Systems). Postprocessing was performed by an experienced observer (R. S. J.) using Circle Cardiovascular Imaging (CVI42; version 5.12.4). Biventricular endocardial and epicardial borders were manually drawn in a stack of short-axis cine images from base to apex in the end-diastolic phase and end-systolic phase to analyze

ventricular volumes, mass, and function. Stroke volume was calculated as end-diastolic volume (EDV)–End-systolic volume (ESV). Ejection fractions were obtained using $SV/EDV \times 100$. Wall masses were computed as diastolic mass + systolic mass/2. Dimensions were indexed (i) to body surface area. Papillary muscles and trabeculae were enclosed in the ventricular wall mass. RV relative wall thickness was calculated as $RV\ mass/RVEDV$.¹³ The feature tracking module of the software was used to obtain RV free wall peak longitudinal strain (RV FWGLS) using the four-chamber cine.

2.3 | PV loop analysis

A single-beat RV PV loop analysis was used to assess the interaction between the RV and PA load (Figure 1).¹⁵ RV end-systolic elastance (Ees), considered a load-independent measure of ventricular contractility, was calculated at rest as $(RV\ maximal\ isovolumic\ pressure\ [RV\ Piso] - RV\ systolic\ pressure\ [RV\ Psys]) / stroke\ volume$.¹⁴ Piso is based on the prediction of maximal pressure if RV contraction remained isovolumic and is a validated technique to determine the maximal isovolumic pressure of the RV.¹⁵ The maximal isovolumetric pressure of the RV was computed by sine wave extrapolation using RV pressure values recorded before the maximal first derivative of pressure development over time (dP/dt) and after minimal dP/dt. RV pressure curves were averaged over multiple beats to reduce respiratory variations. Pulmonary arterial elastance (Ea), considered mainly a reflection of pulmonary vascular resistance (PVR), was calculated as $RV\ Psys / stroke\ volume$.¹⁶ Subsequently, RV pulmonary arterial (RV-PA) coupling was calculated as the ratio of Ees/Ea and represents the efficiency of mechanical energy transfer from the RV to the pulmonary vasculature.¹⁶ RV end-diastolic elastance (Eed) was obtained by fitting a curve through (0,0), the begin-diastolic and end-diastolic points on the PV curve. Eed was calculated as the slope of this curve at end-diastolic volume and represents RV diastolic stiffness.¹⁷

2.4 | CPET

CPET was performed using an electronic braked cycle ergometer according to a standard protocol described before.¹⁸

3 | RESULTS

Eight TGA patients were included (mean age 12 ± 3 years, 75% male) (Table 1). All patients were asymptomatic and all had simple TGA with intact ventricular septum. ASO including a Lecompte maneuver was performed in all patients at a mean age of 6.4 ± 1.8 days and weight of 3.5 ± 0.4 kg. Unilateral PA interventions were performed in the LPA in five out of eight (62%) cases and the RPA in three out of eight cases (38%). None had pulmonary regurgitation.

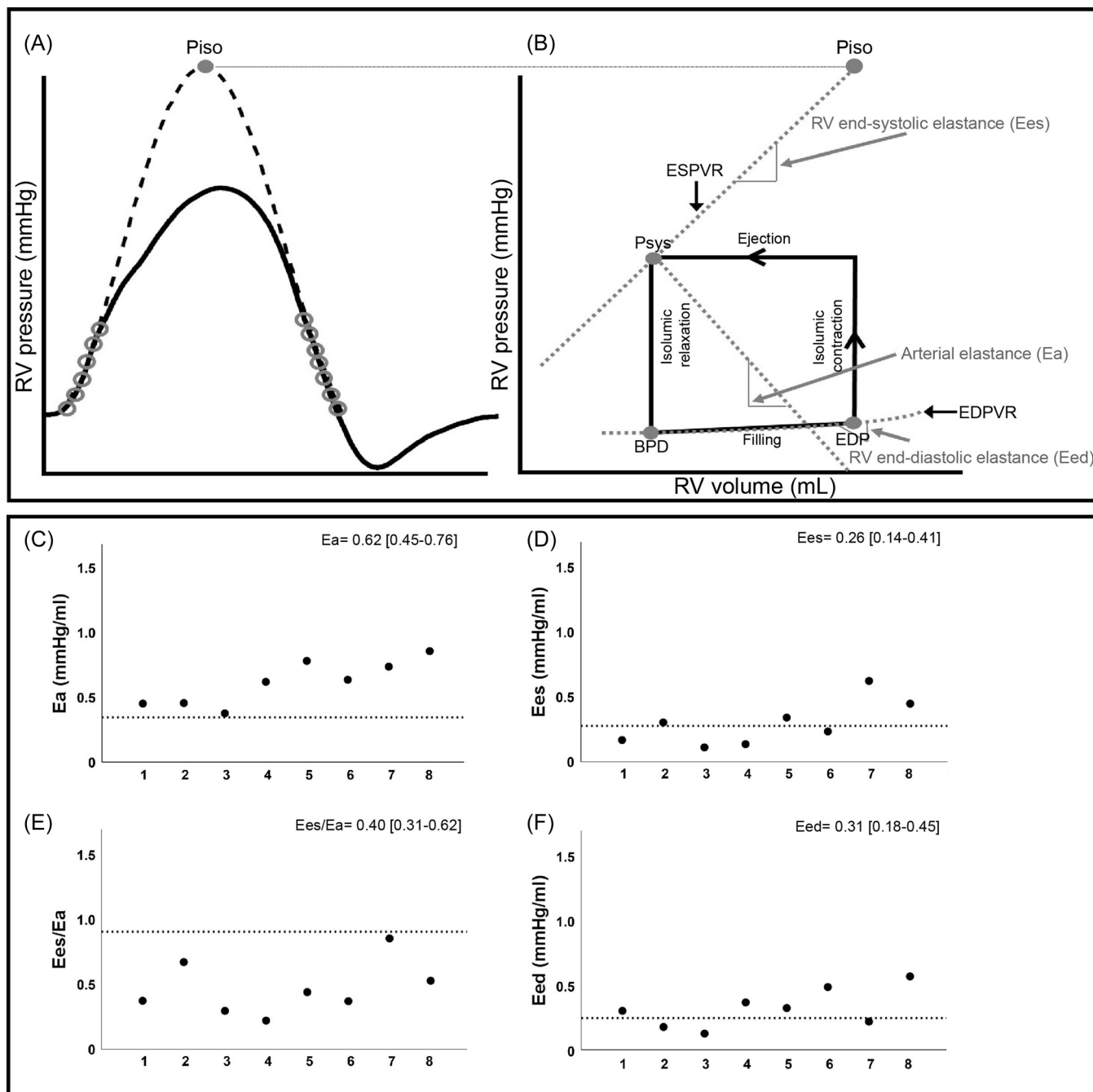


FIGURE 1 Right ventricle (RV) pressure–volume (PV) loop analysis in transposition of the great arteries (TGA) patients with unilateral pulmonary artery stenosis after arterial switch operation (ASO). Schematic example and the individual results of RV PV loop analysis in TGA patients with unilateral PA stenosis after ASO. (A) The maximal isovolumic pressure of the RV (maximal isovolumic pressure [Piso]), used to analyze RV contractility (end-systolic elastanc [Ees]), was computed by sine wave extrapolation using RV pressure values recorded before maximal first derivative of pressure development over time (dP/dt) and after minimal dP/dt.¹⁴ (B) A schematic example of RV PV loop analysis.¹⁵ Arterial elastance (Ea), mainly a reflection of pulmonary vascular resistance, was calculated as RV systolic pressure/stroke volume.¹⁶ Ees, a load-independent measure of ventricular contractility, was calculated as (RV maximal isovolumic pressure–RV systolic pressure)/stroke volume.¹⁴ Right ventricular to pulmonary arterial coupling was calculated as right ventricular to pulmonary arterial coupling and represents the efficiency of energy transfer from the RV to the pulmonary vasculature RV. RV end-diastolic elastance (Eed), used to assess diastolic stiffness, was calculated as the slope of the end-diastolic pressure–volume relationship (EDPVR) at end-diastole.¹⁷ (C–F) Show comparison of Ea (C), Ees (D), Ees/Ea (E), and Eed (F) in TGA patients to normal literature values.^{9,10} BDP, begin-diastolic pressure; EDP, end-diastolic pressure; ESPVR, end-systolic pressure–volume relationship; Psys, RV systolic pressure.

TABLE 2 CMR results.

| Pt | BSA (m ²) | Flow LPA/RPA (%) | LVEDVi (mL/m ²) | LVMi (g/m ²) | LV wall thickness (g/mL) | LVEF (%) | LV GLS (2,3,4-CH) (%) | RVEDVi (mL/m ²) | RVMi (g/m ²) | RV wall thickness (g/mL) | RVEF (%) | RV FWGLS (%) |
|----|-----------------------|------------------|-----------------------------|--------------------------|--------------------------|----------|-----------------------|-----------------------------|--------------------------|--------------------------|----------|--------------|
| 1 | 1.73 | - | 82 | 58 | 0.71 | 63 | -14.1 | 100 | 24 | 0.24 | 46 | -17 |
| 2 | 1.56 | 26/74 | 98 | 54 | 0.55 | 42 | -12 | 119 | 12 | 0.10 | 44 | -17.4 |
| 3 | 1.86 | 29/71 | 92 | 83 | 0.90 | 53 | -12 | 92 | 19 | 0.21 | 47 | -26.3 |
| 4 | 1.03 | 69/31 | 94 | 44 | 0.46 | 62 | -19.5 | 71 | 11 | 0.15 | 68 | -17.1 |
| 5 | 1.36 | 14/86 | 56 | 35 | 0.63 | 66 | -19.4 | 65 | 14 | 0.22 | 60 | -28.7 |
| 6 | 1.07 | 80/20 | 115 | 61 | 0.53 | 65 | -18.9 | 98 | 22 | 0.23 | 66 | -22 |
| 7 | 1.27 | - | 72 | 49 | 0.68 | 49 | -14.4 | 75 | 13 | 0.17 | 46 | -17.8 |
| 8 | 0.95 | 75/25 | 89 | 40 | 0.45 | 61 | -19.1 | 83 | 16 | 0.19 | 59 | -26.3 |

Abbreviations: BSA, body surface area; CMR, cardiac magnetic resonance imaging; FWGLS, free wall global longitudinal strain; GLS, global longitudinal strain; LV, left ventricle; LVEDVi, left ventricular end-diastolic volume indexed; LVEF, left ventricular ejection fraction; LVMi, LV mass indexed; RV, right ventricle; RVEDVi, right ventricular end-diastolic volume indexed; RVEF, right ventricular ejection fraction; RVMi, RV mass indexed.

TABLE 1 Individual characteristics and results heart catheterization.

| Pt | Age (years) | Sex | PA stenosis | NIBP (mmHg) | LV Psys (mmHg) | LV Ped (mmHg) | RV/LV pressure ratio | RVEDP/LVEDP ratio | RV Psys (mmHg) | RV Piso (mmHg) | RV Ped (mmHg) | PAC (mL/mmHg) | LPA gradient (mmHg) | RPA gradient (mmHg) |
|----|-------------|-----|-------------|-------------|----------------|---------------|----------------------|-------------------|----------------|----------------|---------------|---------------|---------------------|---------------------|
| 1 | 15 | M | LPA | 125/65 | 109 | 11 | 0.36 | 0.93 | 39 | 54 | 10 | - | 20 | 0 |
| 2 | 13 | F | LPA | 106/65 | 102 | 13 | 0.28 | 0.73 | 29 | 49 | 10 | 3.86 | 12 | 4 |
| 3 | 16 | M | LPA | 145/65 | 94 | 17 | 0.36 | 0.76 | 34 | 44 | 13 | 4.44 | 9 | 4 |
| 4 | 9 | M | RPA | 104/64 | 95 | 9 | 0.39 | 0.82 | 37 | 45 | 7 | 3.27 | 5 | 15 |
| 5 | 11 | F | LPA | 111/63 | 87 | 8 | 0.45 | 1.03 | 39 | 55 | 8 | - | 17 | 2 |
| 6 | 9 | M | RPA | - | 92 | 15 | 0.54 | 0.91 | 50 | 69 | 14 | 2.69 | 4 | 24 |
| 7 | 12 | M | LPA | - | 83 | 11 | 0.39 | 0.88 | 32 | 59 | 10 | 3.58 | 6 | 1 |
| 8 | 7 | M | RPA | 113/65 | 86 | 17 | 0.51 | 1.06 | 44 | 67 | 18 | 2.61 | 4 | 13 |

Abbreviations: LPA, left PA; LV, left ventricle; LVEDP, left ventricular end-diastolic pressure; NIBP, noninvasive blood pressure; PA, pulmonary artery; PAC, pulmonary artery compliance; Ped, end-diastolic pressure; Piso, maximal isovolumic pressure; Psys, systolic pressure; RPA, right PA; RV, right ventricle; RVEDP, right ventricular end-diastolic pressure.

All patients showed biventricular volumes, masses, ejection fractions, and strain within normal limits after correction for age, gender, and BSA (Table 2). Invasive RV systolic pressures were increased in all TGA patients compared to normal literature values (38 ± 7 vs. 30 mmHg).¹⁹ No pulmonary arterial hypertension was found and pulmonary vein drainage was unaffected in all patients. RV PV loop analysis showed increased RV afterload ($E_a = 0.62$ [0.45–0.76] vs. 0.29 ± 0.05), while RV contractility was decreased ($E_{es} = 0.26$ [0.14–0.41] vs. 0.47 ± 0.20).¹⁰ As a result, RV-PA coupling was severely impaired ($E_{es}/E_a = 0.40$ [0.31–0.62] vs. 1.63 ± 0.74).¹⁰ RV end-diastolic pressures and E_{ed} were increased (Ped: 11 ± 3 vs. 7 mmHg, E_{ed} : 0.31 [0.18–0.45] vs. 0.20 [0.15–0.24]).^{9,19} Invasive LV systolic pressures were within normal limits (94 ± 9 vs. 140 mmHg) while LV end-diastolic pressures were slightly elevated (13 ± 3 vs. 12 mmHg).¹² RV end-diastolic pressures correlated with LV end-diastolic pressures ($R = 0.88$, $p = 0.004$). PAC was mildly reduced (3.4 ± 0.7 vs. 3.8 – 12 mL/mmHg) and

correlated with E_{ed} ($R = 0.97$, $p = 0.002$) (Table 1, Figure 1).¹¹ During a mean follow-up of 6 ± 2 years, all patients remained asymptomatic (New York Heart Association functional class 1) and RV volumes, mass, and systolic function remained unchanged (right ventricular end-diastolic volume indexed: 83 ± 16 mL/m²; RVESVi: 36 ± 8 mL/m²; RV mass indexed: 19 ± 2 g/m²; RV relative wall thickness: 0.24 ± 0.06 g/mL; RVEF: $57 \pm 3\%$; RV FWGLS: $-20 \pm 3\%$). CPET was available in five out of eight patients and showed VO_2 max within normal range after correction for age and weight.

4 | DISCUSSION

This is the first study that describes the effects of unilateral PA stenosis on RV remodeling and function in TGA patients after ASO. We found that (1) RV afterload, estimated by RV pressures and RV

Ea was significantly increased, whereas PAC was decreased. (2) RV volumes, mass, and RVEF remained within normal limits using CMR but (3) RV contractility (Ees) and RV diastolic stiffness (Eed) were compromised leading to RV-PA uncoupling in all patients.

RV afterload and pressures were increased in TGA patients with unilateral PA stenosis after ASO. Increased RV systolic pressure in case of unilateral PA stenosis post-ASO has previously been observed and is particularly interesting since in case of unilateral pulmonary aplasia, PA pressures in the unaffected lung may be normal despite increased blood flow.^{20,21} Subtle gradients without an indication for an intervention in the contralateral PA and a reduced PAC of the PA might contribute to increased systolic RV pressures in these patients. Ea, mainly reflecting PVR, was doubled compared to normal literature values and is in agreement with research in a pig model with unilateral PA stenosis after ASO.²² In addition, PAC was decreased, possibly explained by compromised PA distension in patients with fixed PA stenosis, and might contribute to increased afterload in our patients.²² Despite increased RV afterload, RV remodeling and function remained within normal limits using CMR. This is supported by animal studies showing limited RV hypertrophy in relationship to unilateral PA stenosis.^{22,23} However, we found impaired RV contractility (Ees) and increased RV diastolic stiffness (Eed) using RV PV loop analysis and observed RV-PA uncoupling in all patients. This is substantiated by an animal study that shows reduced RV contractility in the presence of unilateral PA stenosis, which did not restore after the intervention.²² These results may suggest that conventional CMR might not be suitable to detect subclinical RV dysfunction in these patients. Increased RV afterload, decreased RV contractility and subsequently RV-PA uncoupling are also witnessed in other congenital heart diseases.²⁴ LV function was within normal limits and therefore we expect the effect of interventricular interactions on RV function to be limited in our patient group. In addition, despite normal RVEDV, RV Ped and Eed were increased suggesting increased diastolic stiffness and diastolic dysfunction. Previous reports also show RV relaxation abnormalities in the case of preserved RV systolic function in TGA patients after ASO.²⁵ Eed correlated with PAC. Decreased PAC and increased pulse wave velocity might result in increased systolic PA pressures, RV wall stress and increased diastolic stiffness.²⁶ Therefore, increased diastolic stiffness might be the first response to increased afterload in these patients and might even precede systolic dysfunction, as also witnessed in heart failure patients.

4.1 | Clinical implications

Unilateral PA stenosis might result in subclinical RV dysfunction in TGA patients after ASO, while not yet present on CMR. RV volumes, mass and function remained within normal limits during a relatively short follow-up of 6 years. However, the impact of increased afterload over a longer period of time and whether impaired contractility will result in RV maladaptation and ultimately reduced RV function and RV failure remains unknown. Future long-term

studies are needed to 1). assess clinical importance of RV PV loop analysis and 2). to investigate if RV PV loop analysis can be used to assess early predictors for long-term outcomes and to optimize the timing of interventions in these patients.

4.2 | Limitations

Our retrospective study is limited by a small patient population, the use of adult reference values for RV PV loop analysis due to a lack of pediatric reference values and missing PVR data. In addition, RV PV loop analysis was performed using the single-beat method, which is based on assumptions but remains a good and applicable alternative for the multibeat method, which is often unfeasible in patients.¹⁵ Moreover, RV PV loop analysis was only performed at a single time point and does not address the effects of pulmonary interventions on RV-PA coupling. This is currently being investigated in a multicenter randomized controlled trial in patients with biventricular CHD ([ClinicalTrials.gov](https://clinicaltrials.gov) ID: NCT05809310).

5 | CONCLUSION

Unilateral PA stenosis results in an increased RV afterload in TGA patients after ASO. RV remodeling and function remain within normal limits when analyzed by CMR but RV PV loop analysis show impaired RV diastolic stiffness and RV contractility leading to RV-PA uncoupling.

ACKNOWLEDGMENTS

We thank J. de Rover for his assistance and contribution to this article. We acknowledge the support from the Netherlands Cardiovascular Research Initiative to this article as the funding source for Renée S. Joosen her Project as part of the OUTREACH consortium: an initiative with the support of the Dutch Heart Foundation and Hartekind, CVON2019-002 OUTREACH. M. Louis Handoko is supported by the Dutch Heart Foundation (2020T058) and CVON (2020B008).

CONFLICT OF INTEREST STATEMENT

M. Louis Handoko received an educational grant from Novartis and Boehringer Ingelheim, and speaker/consultancy fees from Novartis, Boehringer Ingelheim, Daiichi Sankyo, Vifor Pharma, AstraZeneca, Bayer, MSD, Abbott, and Quin. The remaining authors declare no conflict of interest.

DATA AVAILABILITY STATEMENT

The data underlying this article will be shared upon reasonable request to the corresponding author.

ORCID

Renée S. Joosen  <http://orcid.org/0000-0001-8262-923X>

Gregor J. Krings  <http://orcid.org/0000-0002-2453-3181>

REFERENCES

1. van der Palen RLF, Blom NA, Kuipers IM, et al. Long-term outcome after the arterial switch operation: 43 years of experience. *Eur J Cardiothorac Surg*. 2021;59(5):968-977.
2. Giardini A, Khambadkone S, Taylor A, Derrick G. Effect of abnormal pulmonary flow distribution on ventilatory efficiency and exercise capacity after arterial switch operation for transposition of great arteries. *Am J Cardiol*. 2010;106(7):1023-1028.
3. Geva T, Sandweiss BM, Gauvreau K, Lock JE, Powell AJ. Factors associated with impaired clinical status in long-term survivors of tetralogy of Fallot repair evaluated by magnetic resonance imaging. *J Am Coll Cardiol*. 2004;43(6):1068-1074.
4. Valente AM, Gauvreau K, Assenza GE, et al. Contemporary predictors of death and sustained ventricular tachycardia in patients with repaired tetralogy of Fallot enrolled in the INDICATOR cohort. *Heart*. 2014;100(3):247-253.
5. Egbe AC, Kothapalli S, Borlaug BA, et al. Mechanism and risk factors for death in adults with tetralogy of Fallot. *Am J Cardiol*. 2019;124(5):803-807.
6. Brenner MI, Masoumi A, Ng VG, et al. Invasive right ventricular pressure-volume analysis: basic principles, clinical applications, and practical recommendations. *Circ Heart Fail*. 2022;15(1):e009101.
7. van der Ven JPG, Sadighy Z, Valsangiacomo Buechel ER, et al. Multicentre reference values for cardiac magnetic resonance imaging derived ventricular size and function for children aged 0-18 years. *Eur Heart J Cardiovasc Imaging*. 2020;21(1):102-113.
8. Qu YY, Li H, Rottbauer W, Ma GS, Buckert D, Rasche V. Right ventricular free wall longitudinal strain and strain rate quantification with cardiovascular magnetic resonance based tissue tracking. *Int J Cardiovasc Imaging*. 2020;36(10):1985-1996.
9. Wessels J, Mouratoglou SA, Van Wezenbeek J, et al. Right ventricular stiffness impairs right atrial function in pulmonary arterial hypertension. *Eur Respir J*. 2020;56:4047.
10. Spruijt OA, de Man FS, Groepenhoff H, et al. The effects of exercise on right ventricular contractility and right ventricular-arterial coupling in pulmonary hypertension. *Am J Respir Crit Care Med*. 2015;191(9):1050-1057.
11. Thenappan T, Prins KW, Pritzker MR, Scandurra J, Volmers K, Weir EK. The critical role of pulmonary arterial compliance in pulmonary hypertension. *Ann Am Thorac Soc*. 2016;13(2):276-284.
12. Cornelissen HAJ. Preoperative assessment for cardiac surgery. *Crit Care Pain*. 2006;6:109-113.
13. Gaasch WH, Zile MR. Left ventricular structural remodeling in health and disease. *J Am Coll Cardiol*. 2011;58(17):1733-1740.
14. Suga H, Sagawa K, Shoukas AA. Load independence of the instantaneous pressure-volume ratio of the canine left ventricle and effects of epinephrine and heart rate on the ratio. *Circ Res*. 1973;32(3):314-322.
15. Brimioule S, Wauthy P, Ewalenko P, et al. Single-beat estimation of right ventricular end-systolic pressure-volume relationship. *Am J Physiol Heart Circ Physiol*. 2003;284(5):H1625-H1630.
16. Sunagawa K, Maughan WL, Sagawa K. Optimal arterial resistance for the maximal stroke work studied in isolated canine left ventricle. *Circ Res*. 1985;56(4):586-595.
17. Trip P, Rain S, Handoko ML, et al. Clinical relevance of right ventricular diastolic stiffness in pulmonary hypertension. *Eur Respir J*. 2015;45(6):1603-1612.
18. Baggen VJM, Driessen MMP, Meijboom FJ, et al. Main pulmonary artery area limits exercise capacity in patients long-term after arterial switch operation. *J Thorac Cardiovasc Surg*. 2015;150(4):918-925.
19. Lampert BC. *Right Heart Catheterization*. Elsevier; 2018.
20. Hiremath G, Qureshi AM, Prieto LR, et al. Balloon angioplasty and stenting for unilateral branch pulmonary artery stenosis improve exertional performance. *JACC Cardiovasc Interv*. 2019;12(3):289-297.
21. Jariwala P, Maturu VN, Christopher J, Jadhav KP. Congenital isolated unilateral agenesis of pulmonary arteries in adults: case series and review. *Indian J Thorac Cardiovasc Surg*. 2021;37(suppl 1):144-154.
22. Bates ML, Anagnostopoulos PV, Nygard C, et al. Consequences of an early catheter-based intervention on pulmonary artery growth and right ventricular myocardial function in a pig model of pulmonary artery stenosis. *Catheter Cardiovasc Interv*. 2018;92(1):78-87.
23. Pewowaruk R, Hermsen J, Johnson C, et al. Pulmonary artery and lung parenchymal growth following early versus delayed stent interventions in a swine pulmonary artery stenosis model. *Catheter Cardiovasc Interv*. 2020;96(7):1454-1464.
24. Latus H, Binder W, Kerst G, Hofbeck M, Sieverding L, Apitz C. Right ventricular-pulmonary arterial coupling in patients after repair of tetralogy of Fallot. *J Thorac Cardiovasc Surg*. 2013;146(6):1366-1372.
25. Grotenhuis HB, Kroft LJM, van Elderen SGC, et al. Right ventricular hypertrophy and diastolic dysfunction in arterial switch patients without pulmonary artery stenosis. *Heart*. 2006;93(12):1604-1608.
26. Vonk-Noordegraaf A, Haddad F, Chin KM, et al. Right heart adaptation to pulmonary arterial hypertension. *J Am Coll Cardiol*. 2013;62(25 suppl):D22-D33.

How to cite this article: Joosen RS, Voskuil M, Krings GJ, et al. The impact of unilateral pulmonary artery stenosis on right ventricular to pulmonary arterial coupling in patients with transposition of the great arteries. *Catheter Cardiovasc Interv*. 2024;103:943-948. doi:10.1002/ccd.31036